Supporting Information

Sanchez et al. 10.1073/pnas.1306467110

SI Materials and Methods

Proteins, DNA Substrates, and Fluorescent Fiducials. Human RAD51 and a his6-tagged version of human RAD54 protein were purified as described (1). RAD54 was cloned in a pFASTBAC1 vector (Invitrogen) in frame with the AviTag sequence (2). Recombinant Baculovirus vector containing RAD54-avitag (His6-hRAD54-bio) was used for co-infecting Sf21 or Sf9 insect cells along with baculovirus encoding the BirA biotin ligase. Insect cells were cultured in the presence of 2 μM biotin. The biotinylated version of RAD54 was purified following the same protocol as the non-biotinylated protein. ATPase hydrolysis of the proteins in the presence of DNA was performed as previously described (3).

Linear dsDNA (1 kbp) molecules were generated by PCR amplification of pBluescript DNA with 5′-AF647 GCT GAG TGA TAT CCC GCT TAA C-3′ and 5′-CCA CCA CTT CAA GAA CTA-3′ or by PCR amplification of bacteriophage M13mp18 dsDNA with 5′-TGA GGG TGG CGG TAC TAA AC-3′ and 5′-CCC AAA AGA ACT GGC ATG AT-3′. Linear ssDNA (1 kb) molecules were generated by PCR amplification of pBluescript DNA with a phosphorothioate modified oligo 5′-TsGsAsGsGsGs TGG CGG TAC TAA AC-3′ and 5′-CCC AAA AGA ACT GGC ATG AT-3′ and degradation of the unprotected strand with lambda exonuclease I.

We used TransFluoSpheres [0.04 μm diameter (488/645); Invitrogen] as fiducials markers, and AlexaFluor-633 (632/647) conjugated streptavidin (Molecular Probes), which we determined to contain 2.7 dye molecules per tetramer, for labeling RAD54.

1. Swagemakers SM, Essers J, de Wit J, Hoeijmakers JH, Kanaar R (1998) The human RAD54 recombinational DNA repair protein is a double-stranded DNA-dependent ATPase. *J Biol Chem* 273(43):28292–28297.
2. Schatz PJ (1993) Use of peptide libraries to map the substrate specificity of a peptide-modifying enzyme: a 13 residue consensus peptide specifies biotinylation in Escherichia coli. *Biotechnology* (*N Y*) 11(10):1138–1143.
3. Sanchez H, Suzuki Y, Yokokawa M, Takeyasu K, Wyman C (2011) Protein-DNA interactions in high speed AFM: single molecule diffusion analysis of human RAD54. *Integr Biol* (*Camb*) 3(11):1127–1134.

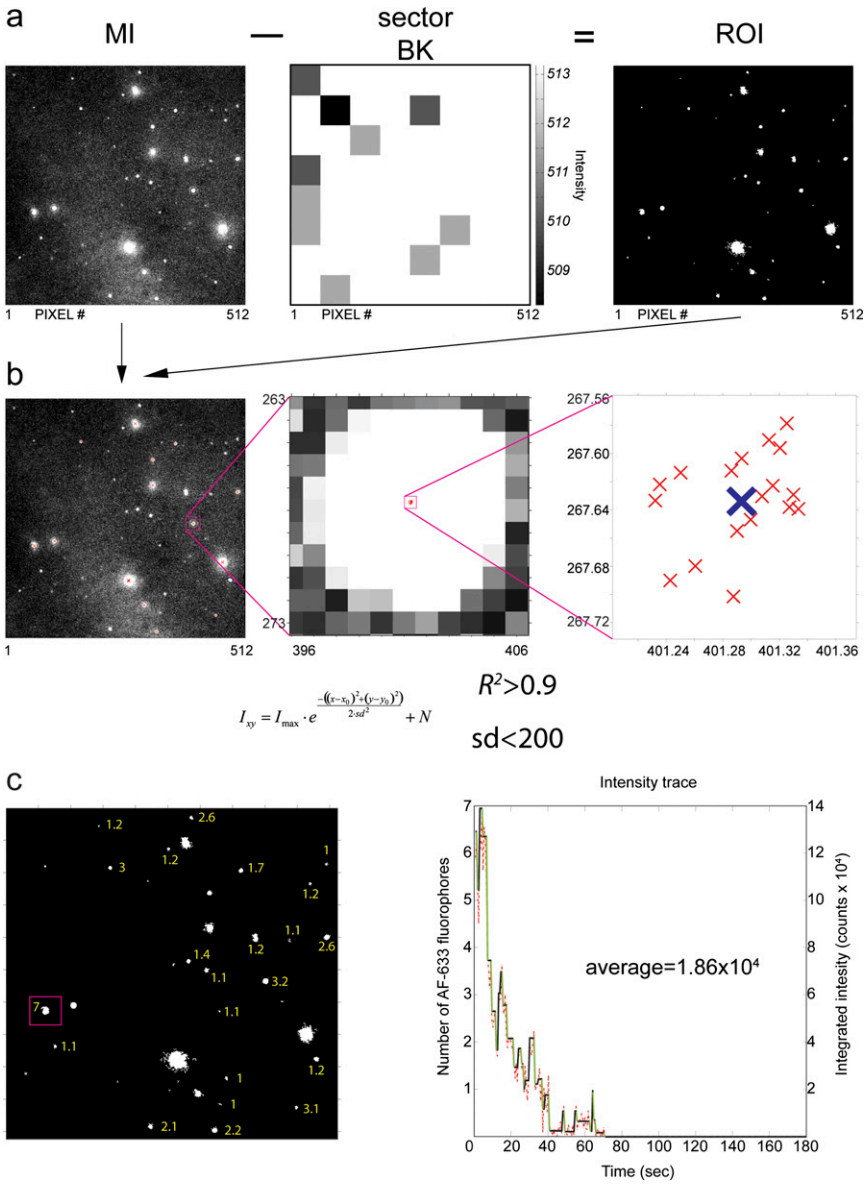

Fig. S1. Image processing of total internal reflection fluorescence (TIRF) pictures. (*A*) Detection of regions of interest (ROI). We used the Template Matching plug-in developed by Q. Tseng (available at https://sites.google.com/site/qingzongtseng/template-matching-ij-plugin) for alignment of the images. The images were aligned between each other by normalized cross-correlation of pixel intensity of a defined pattern in the image. This stack of images was used to create a maximum intensity composite (MI). Stacks were then opened in MATLAB with tiffread2.m, developed by F. Nedelec (available at www.cytosim.org/other/). MI is corrected for uneven illumination with a sectorized background (sector BK); the result is a binary mask with the ROIs (white pixels). *x* axis, pixel number. (Scale bar, intensity counts.) (*B*) Subpixel localization of fluorescent human homologous recombination protein RAD54. The intensity of the pixels contained in each ROI was fit with a 2D Gaussian function to find its center of mass (x_0, y_0). Only positions with SD smaller than 200 nm and fits with a determination coefficient (R^2) higher than 0.9 were considered for constructing the localization cluster. I_{xy}, total intensity of the ROI; I_{max}, maximum intensity; *N*, noise; *x* and *y*, coordinates of individual pixels inside the ROI. (*Left*) MI overlaid with the localization cluster of each ROI (red crosses). One ROI is highlighted with the pink square and zoomed in the central and right panels. *x* and *y* axis, pixel number. Blue cross in the right panel is the centroid of the localization cluster. One pixel equals 62 nm. (*C*) Counting fluorophores using the stepwise bleaching and blinking of single Alexa Fluor 633 conjugate–streptavidin. *Left* shows the same ROI-image as in *A* and *B,* with the number of estimated fluorophores per ROI in yellow. One ROI is highlighted with a pink square, and the analysis of its intensity trace is shown in *Right*. Intensity over time of the measured ROIs fluctuated as a consequence of fluorophore blinking, fluorophore bleaching, and subtle changes in illumination conditions between frames. The intensity per frame, plotted as a red dashed line, was fit with a step finding algorithm (32, 33), plotted as a black and green line. The average down step-size (green lines), the fluorescence difference between on and off fluorophore state, was used to calculated the total number of fluorophores per ROI.

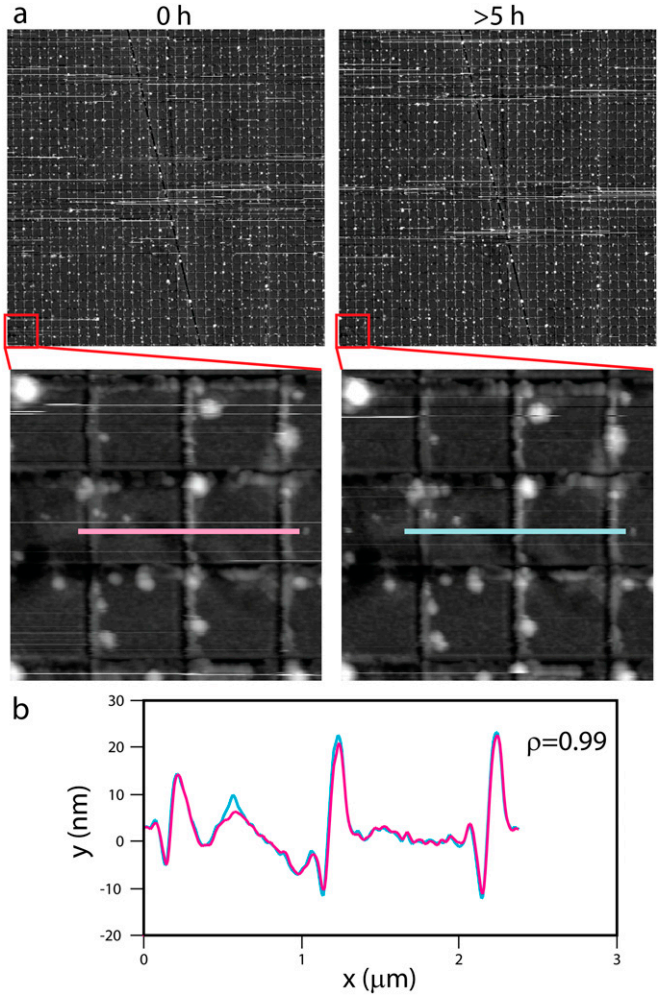

Fig. S2. Scanning force microscope (SFM) images are unaffected by drift while scanning. A silicon-dioxide grid with 1 μm pitch was scanned in the same conditions as the RAD54 samples: 35 × 35 μm (4,096 × 4,096 pixels) at a line rate of 0.2 Hz. (*A, Upper*) Images of consecutive scans. (*Lower*) Zoomed images of the region highlighted in the red square. (*B*) Height profile of the pixels in the lines drawn in *A*. The high value of the Pearson correlation (ρ) between the pixel intensity of the lines indicated the absence of drift between the two images.

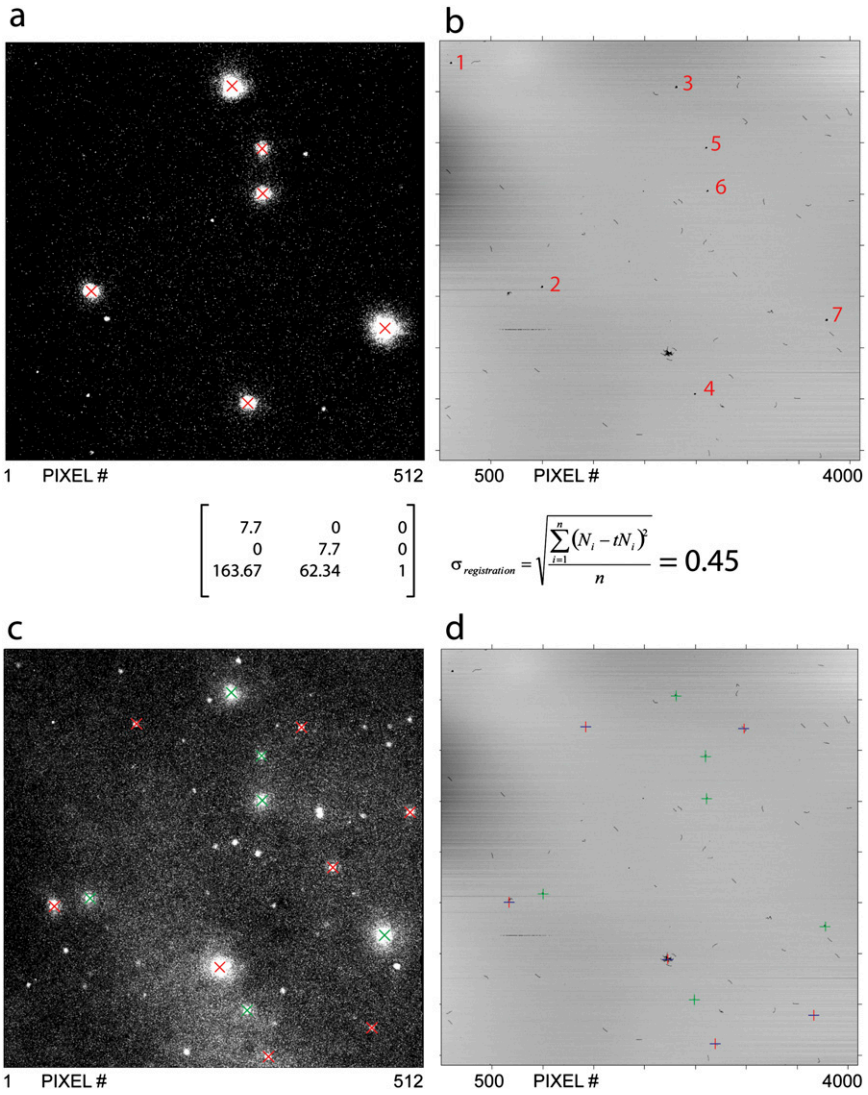

Fig. S3. Registration of TIRF and SFM images. (*A*) TIRF image of fluorescent fiducials after excitation with the 488-nm laser. The centroid positions of the localization cluster (red cross) are overlaid. *x* axis, pixel number. (*B*) SFM image of the TIRF image shown in *A* overlaid with numbered fiducials. *x* and *y* axis, pixel number. Fiducials numbered 2–6 were used to match the position of the centroids in *A* to obtain the transformation matrix and associated uncertainty ($\sigma_{registration}$). The TIRF image is 10.56 μm^2 smaller than the SFM image, so the fiducial number 1 is not visible. (*C*) TIRF image of labeled RAD51–dsDNA–RAD54 complexes after excitation with the 633-nm laser. The centroid positions of the localization cluster (red crosses) were overlaid. Fluorescent fiducials (green crosses) are also detected with the 633 nm but with lower intensity than in *A*. *x* axis, pixel number. (*D*) SFM image of the TIRF image in *C* with the centroid positions of the localization cluster (red and blue crosses) of RAD54 overlaid after applying the transformation matrix; the size of the crosses are not at scale, as in Fig. 5. *x* and *y* axis, pixel number.

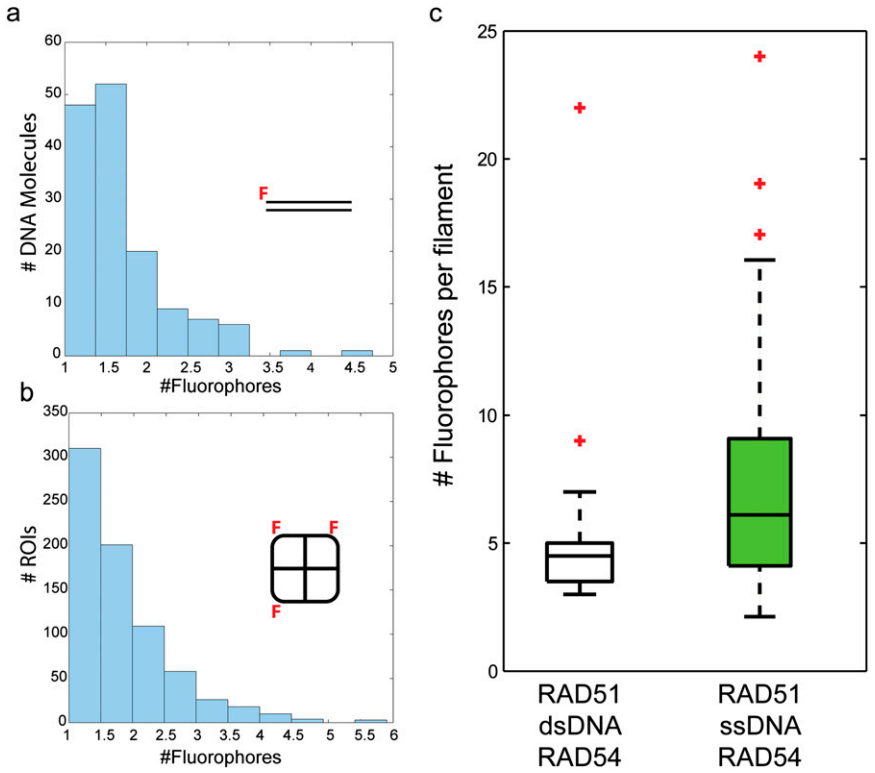

Fig. S4. Accurate quantification of fluorophores in labeled DNA and proteins. (*A*) Distribution of the number of fluorophores per DNA molecule. Fluorescence intensity was measured for each DNA molecule over time. Using a step-fitting algorithm, the number of fluorophores per DNA was calculated (Fig. S1*C*). The cartoon represents a labeled dsDNA molecule. (*B*) Distribution of the number of fluorophores per streptavidin tetramer. The cartoon represents a labeled streptavidin tetramer. ROIs, regions of interest. (*C*) Box plots of the number of fluorophores detected in class 3 complexes with RAD51–dsDNA (white box, $n = 32$) and RAD51–ssDNA (green box, $n = 77$). Red line, median; the edges of the box are the 25th and 75th percentiles, and the whiskers extend to the most extreme data points not considered outliers (red crosses).

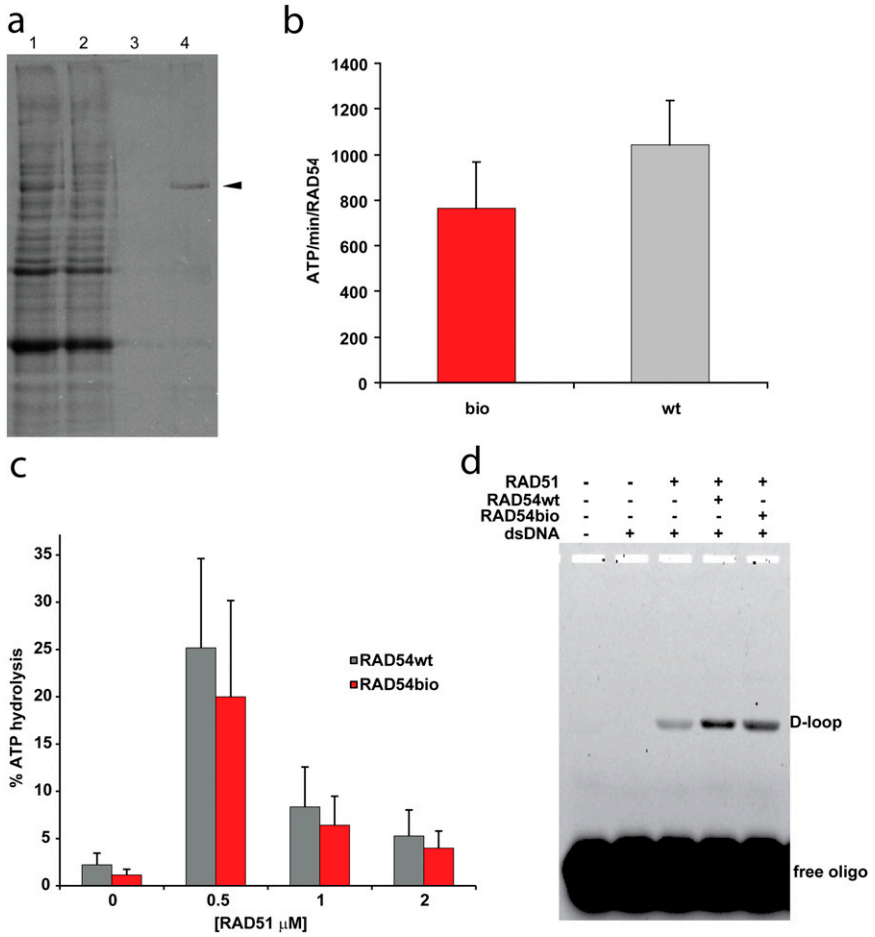

Fig. S5. Characterization of biotinylated RAD54. (*A*) Biotinylated RAD54 present in the cell extract binds specifically to streptavidin beads. Coomassie-stained SDS-PAGE gel of biotinylated RAD54 protein extracts before and after beads treatment. Lane 1, extract from insect cells, expressing hRAD54avitag and BirA biotin ligase in the presence of biotin, after phosphocellulose chromatography, used for incubation with Dynabeads M-280 streptavidin (Invitrogen); lane 2, flow-through (unbound) material from the beads after 30 min incubation at room temperature; lane 3, material in a wash step from the beads; lane 4, bead-bound proteins (i.e., RAD54bio). (*B*) Biotinylated RAD54 (bio) retains ATPase activity similar to the nonbiotinylated (wt) protein in the presence of supercoiled dsDNA. Error bars are the SE ($n = 3$). (*C*) Biotinylated RAD54 ATPase activity is stimulated by partially coated RAD51–dsDNA complexes. The indicated amount of RAD51 was incubated with dsDNA (2 μM in bp of pUC19 plasmid DNA) in reaction buffer (50 mM Tris·HCl at pH 7.5, 1 mM DTT, 0.1 mg/mL acetylated BSA, 60 mM KCl, 2 mM CaCl2, and 1 mM ATP containing 10 nM [γ^{32}P] ATP) in the presence of RAD54wt or RAD54bio (60 nM). After 5 min incubation at 30 °C, reaction was stopped with EDTA (50 mM) and kept in dry ice until the reaction products were analyzed by TLC. Error bars are the SE ($n = 3$). (*D*) Biotinylated RAD54 enhances RAD51-mediated DNA strand invasion. In vitro formation of displacement loops (D-loops) were made by incubating human RAD51 protein (2 μM) in a final volume of 10 μL with 5′-end Alexa Fluor 488–labeled 90 nt ssDNA (AF488SK3$_{ss}$) at 3.6 μM (nt), in reaction buffer. After 5 min incubation at 30 °C, 1 μL supercoiled pUC19 plasmid DNA at 1.1 mg/mL (purified by double cesium chloride density gradient centrifugation) and further incubated for 20 min at 30 °C. Samples were deproteinized by adding SDS (1%), EDTA (25 mM), and Proteinase K (1 μg/μL) and incubated for 5 min at 37 °C. Reaction mixtures were resolved by 0.7% agarose gel electrophoresis in 0.5× TB buffer. Gels were analyzed using a Typhoon Trio scanner (GE Healthcare).